International Journal of Thermophysics (2021) 42:155
https://doi.org/10.1007/s10765-021-02908-8

A Study of $LiNO_3$–NaCl/EG Composite PCM for Latent Heat Storage

Y. Li[1] · W. C. Tie[1] · Q. Z. Zhu[1] · Z. Z. Qiu[1]

Received: 8 June 2021 / Accepted: 7 August 2021 / Published online: 18 August 2021

Abstract

To find a medium temperature phase change heat storage material with high thermal conductivity and heat storage ability, expanded graphite (EG) with high thermal conductivity is used as the carrier material, and the binary mixed molten salt of 88 wt% $LiNO_3$–12 wt% NaCl is used as the phase change material (PCM). EG and PCM are uniformly dispersed by ultrasound crushing method. To get the right EG addition ratio, $LiNO_3$–NaCl/EG composite PCMs (LNE) with EG mass ratio of 10 %, 15 %, 20 %, and 30 % are prepared by static melt adsorption method. The melting point, phase change enthalpy and other parameters of the composite material are tested and analyzed. The experimental results show that the melting temperature and the phase change enthalpy of LNE gradually decrease with the increase of EG mass proportion. For all LNE samples, the adsorption ratio of PCM exceeds 90 % to 95 %. The thermal conductivity of the PCM greatly improves with the increase of EG mass proportion. The thermal conductivity of the composites with 15 wt% EG is 6.532 $W{\cdot}m^{-1}{\cdot}K^{-1}$, which is about 3.7 times that of the binary mixed molten salt. The thermal conductivity increases with the increase of the apparent density. The composite PCM has stable performance. The 85 wt% $LiNO_3$–NaCl/15 wt% EG composite PCM has the best overall performance.

Keywords Adsorption ratio · Composite phase change material · Phase change latent heat · Thermal conductivity · Thermal stability

✉ Y. Li
yli@shiep.edu.cn

✉ Q. Z. Zhu
zhuqunzhi@shiep.edu.cn

[1] College of Energy and Mechanical Engineering, Shanghai University of Electric Power, Shanghai 200090, China

1 Introduction

With the development of society's awareness of environmental protection, heat storage technology is becoming increasingly important. Inorganic phase change heat storage materials are widely used because of their wide temperature range, high latent heat of phase change and low cost [1, 2]. But they usually have following problems: low thermal conductivity, certain supercooling degree, and easy to leak during the phase change process [3]. The mainstream method of improving thermal conductivity of heat storage materials is adding materials with high thermal conductivity, such as metal oxide and non-oxide nanoparticles [4–6], graphene [7], expanded graphite (EG) [8–10], etc. The porous material matrix can soak PCM in the pores or channels. Due to the interaction of capillary force, PCM can be effectively absorbed in a closed space [11]. The liquid leakage problem of the solid–liquid phase change material (PCM) will then be solved. EG has a porous structure and high thermal conductivity, and the price is relatively low, which has attracted wide attention.

EG has been combined with various organic and inorganic PCM to prepare composite PCM [12–15]. Li et al. [16] prepared $NaNO_3$–$LiNO_3$/EG composite PCMs and found that EG does not significantly affect the melting temperature of composite PCMs, but the phase change latent heat gradually decreases with the increase of EG mass proportion. The thermal conductivity increases with the increase of the molding pressure and EG mass proportion. The sample with fewer EG mass proportion has better thermal stability. Zhao et al. [17] prepared paraffin/EG shaped composite PCMs and investigated the effect of EG size on the structure and properties of EG-based paraffin composite PCM. The test results reveals that large EG-based matrix has a higher porosity and a larger pore size compared with small EG-based matrix. The different structural characteristics of the EG has a great impact on paraffin uptake, and hence affects the thermal properties of the EG/paraffin composites.

Thermal energy-storage capacity is an imperative parameter of composite PCM. The energy-storage/release performance of a phase change composite depends on the loading of the composite components [18]. Feng et al. [19] successfully synthesized hierarchical porous carbon (HPC) from metal organic framework MOF-5 with a large specific surface area and high pore volume. The adsorption capacity of HPC for low temperature PCM reaches over 90 wt%. The composites possess similar high thermal storage capacity to pure PCM. In addition to the adsorption effect of EG on the heat storage material, the heat storage capacity of the heat storage material itself has a greater influence on the heat storage capacity of the EG composite heat storage material. Li et al. [20, 21] prepared $LiNO_3$–KNO_3/EG composite PCM, and analyzed its thermophysical properties and thermal reliability. The results show that EG can effectively improve the thermal conductivity of heat storage materials, and the performance is stable. But the latent heat of fusion of $LiNO_3$-KNO_3 is 170.2 $J \cdot g^{-1}$, which is relatively low, and it is necessary to carry out research on materials with higher heat storage capacity.

The latent heat of fusion of 88 wt% $LiNO_3$–12 wt% NaCl solid–liquid PCM is as high as 389.3 $J \cdot g^{-1}$, and the phase transition temperature is 222.6 ℃ [22]. It is

a kind of medium temperature heat energy-storage material with good application prospect, but it still has the problem of low thermal conductivity. Because the carrier material does not have the heat storage capability, its addition reduces the heat storage capacity of the whole material. Therefore, it is necessary to understand the influence of the addition of EG on the heat storage capacity and thermal conductivity of materials. For solid–liquid PCMs, it is necessary to select an appropriate proportion of EG to ensure that they do not leak during the phase transition. In this paper, 88 wt% $LiNO_3$–12 wt% NaCl is used as phase change heat storage material. EG is used as carrier. LNE with different mass ratios of EG were prepared. The microstructure, phase transition temperature, phase change latent heat, and the effective thermal conductivity were tested and analyzed. This work aims to obtain the optimal ratio of LNE materials, and to explore the middle-temperature shaped composite heat storage materials with high thermal conductivity and high heat storage density.

2 Materials and Methods

2.1 Preparation of Materials

$LiNO_3$, NaCl and EG are used to prepare LNE. The raw material information is shown in Table 1. The phase change temperature and phase change latent heat of $LiNO_3$ and NaCl are all measured values.

EG was prepared using high-temperature expansion method. Some expandable graphite was put in a constant temperature drying oven (80 ℃) for 24 h to remove moisture, then moved to corundum porcelain boat and put in the muffle furnace about 800 ℃ for 1–2 min to get EG.

$LiNO_3$–NaCl binary mixed molten salt and EG were put into a constant temperature drying oven (120 ℃) for 24 h to remove the moisture, then poured into deionized water for 10 min. The percentage of EG in the total mass was 10 %, 15 %, 20 %, 30 %. The mixed solution was stirred by ultrasonic cell crusher for 5 min before being put into a constant temperature drying oven (80 ℃), until reaching "sticky"

Table 1 Experimental materials

Name	Type	Melting temperature/℃	Latent heat/J·g^{-1}	Expansion ratio/mL·g^{-1}	Manufacturer
$LiNO_3$	AR ≥ 99.0 %	255	362		Shanghai Feng shun Chemical Co., Ltd
NaCl	GR ≥ 99.9 %	801	492		Sinopharm Chemical Reagent Co., Ltd
Expandable graphite	Mesh 50			90–120	Shanghai Yi-fang Graphite Co., Ltd

state. It was then put into the muffle furnace at 300 ℃ for 120 min, then removed and cooled to get the composite thermal storage material.

2.2 Characterization Techniques

2.2.1 X-ray Powder Diffraction (XRD) Test

D/Max-2550VB/PC type X-ray diffractometer (Rigaku Company, Japan) was used in the XRD test to study the compatibility of the binary molten salt and EG, CuKα as a radiation source. The wavelength was 0.15406 nm and the scan angle was 10°–90°.

2.2.2 Phase Change Behavior Analysis

The melting point and latent heat of the material were analyzed by Mettler TGA/DSC2 1600 thermogravimetric analyzer and synchronous thermal analyzer (Switzerland METTLER Toledo Company). The DSC test condition for $LiNO_3$–KNO_3/EG composite PCMs was as follows: the heating and cooling rate was 10 °C·min^{-1} within a temperature range of 100–300–100 ℃, and the temperature was kept for 5 min at 300 ℃. The atmosphere here was argon and its flow rate was 20 mL·min^{-1}.

2.2.3 Thermal Conductivity Measurement

The thermal conductivity of composite PCM was tested by Hot Disk TPS 2500 s thermal constant analyzer (Hot Disk Company, Sweden) using transient plane heat source method. The sample temperature changed with time in the process of test. The samples were pressed into thin chip by SFLS-5 powder tablet machine and tested.

2.2.4 Thermal Stability Analysis

The composite PCM with 85 wt% $LiNO_3$-NaCl/15 wt% EG was selected for the cyclic thermal stability test. The DSC test conditions for cyclic thermal stability were as follows: the heating temperature range was 100–300–100 ℃, the heating and cooling rate was 10 ℃·min^{-1}. The protective atmosphere was nitrogen, and the gas flow rate was 20 mL·min^{-1}.

3 Results and Discussion

3.1 XRD Test Results

Figure 1 shows the XRD diagrams of EG and LNE. By comparing the standard cards, the characteristic peaks of $LiNO_3$, KNO_3 and EG do not change. It demonstrates that the crystal structure does not change during the process of preparation,

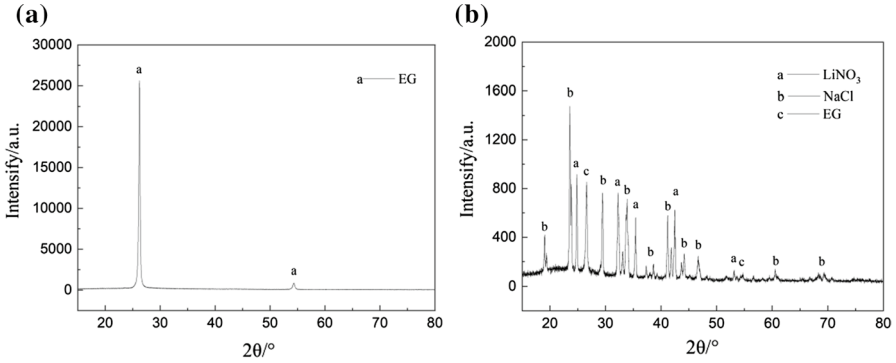

Fig. 1 XRD diagram of EG and LNE (a) EG (b) LNE

and there is no chemical reaction even under the high-temperature molten state. The materials have good thermal and chemical stability. The preparation method is reliable.

3.2 Phase Change Behaviors of Composite PCM

Figure 2 shows DSC curves of $LiNO_3$–KNO_3/EG composite PCMs with EG at mass proportion of 5 %, 10 %, 15 %, 20 %, and 30 %, respectively. The melting temperature, melting peak temperature, melting latent heat, solidification temperature, solidification peak temperature, and solidification latent heat are obtained by DSC curve analysis. The detailed values are shown in Table 2. For the convenience of analysis and comparison, DSC test result of $LiNO_3$–NaCl is also given in Fig. 2 and Table 2. For heating melting process, the melting temperature of the sample with 10 wt% EG is almost the same with the melting temperature of the mixed molten salt. The endothermic melting temperature of the other composite PCMs is 2.3–3.5 ℃ lower than $LiNO_3$–NaCl binary mixed molten salt. This may be due to changes in particle size.

In general, smaller grain size means less crystallization degree and lower melting point. Larger grain size corresponds to better crystallization degree and higher melting point [13]. The addition of EG has the effect of heterogeneous nucleation, more nucleation points reduce the grain size of the mixed molten salt, then reduces the melting temperature of composite PCMs. For the composite PCMs of 10 wt% EG, $LiNO_3$–NaCl mixed molten salt is in excessive state and has not been completely absorbed by EG porous structure. Its basic performance is the same with $LiNO_3$–NaCl binary mixed molten salt in the melting process.

With the increase of EG mass proportion, excessive $LiNO_3$–NaCl mixed molten salt can also be absorbed by the pore structure of EG. The crystal surface area of the mixed molten salt increases, the crystal size decreases. Also, the melting temperature of composite PCM decreases to about 221 ℃. It demonstrates that excessive EG has little impact on the melting temperature of composite PCM after reaching saturation of EG pore structure.

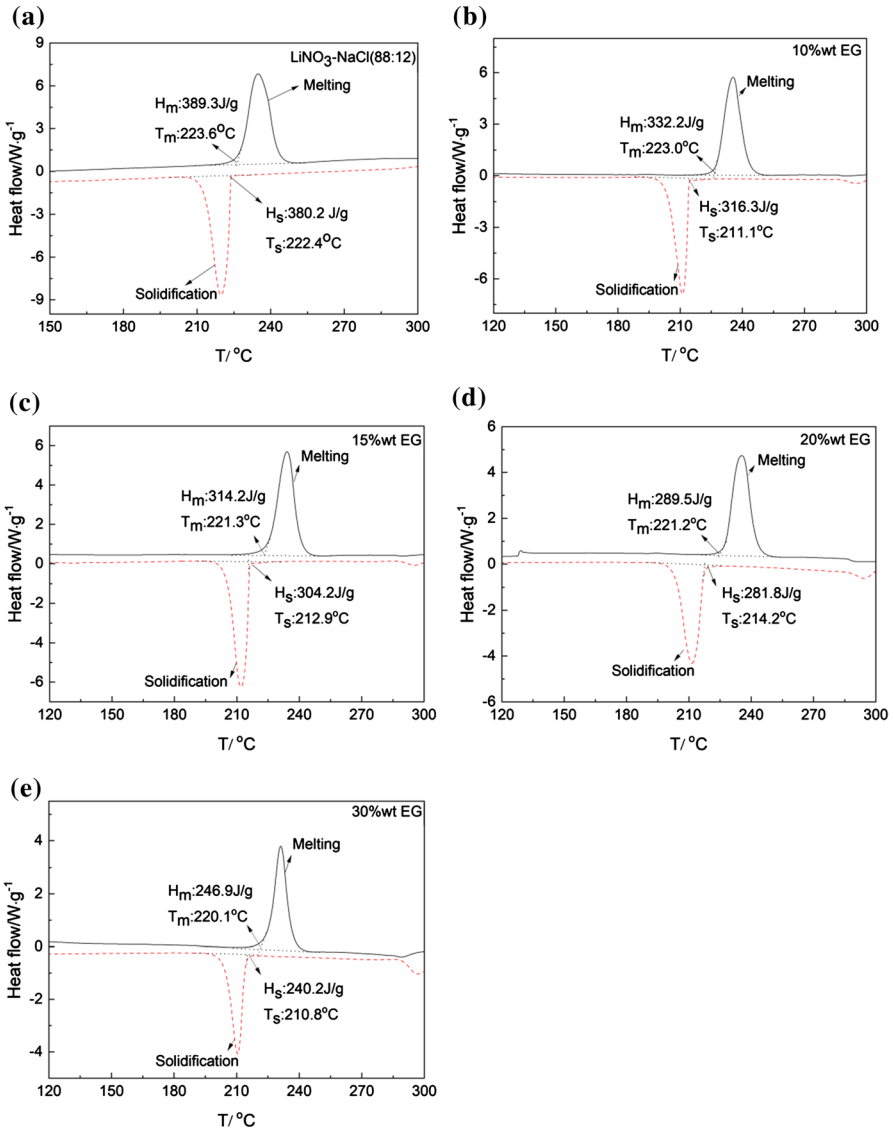

Fig. 2 DSC curves of the composites with different EG mass proportion (a) 0 %EG (b) 10 %EG (c) 15 %EG (d) 20 %EG (e) 30 %EG

As shown in Fig. 2, the angle between the tangent from inflexion point of endothermic peak start edge and the baseline tends more to right angle for the composites, than that of $LiNO_3$–NaCl binary mixed molten salt. The endothermic peak is more acute. It shows that the phase change rate of the composites is faster. The possible reason is that the porous layer structure of EG provides channels to enhance heat transfer. At the same time, the stripped graphite pieces produced by strong

Table 2 The thermal physical parameters of $LiNO_3$–KNO_3/EG composites

EG mass proportion (%)	The melting process			The solidification process		
	T_m (℃)	$T_{peak\text{-}m}$ (℃)	H_m (J·g^{-1})	T_s (℃)	$T_{peak\text{-}s}$ (℃)	H_s (J·g^{-1})
0	223.6	235.1	389.3	222.4	220.0	380.2
10	223.0	229.8	332.2	211.1	209.6	316.3
15	221.3	228.5	314.2	212.9	210.3	304.2
20	221.2	230.5	289.5	214.2	209.3	281.8
30	220.1	227.4	246.9	210.8	206.4	240.2

ultrasonic strengthen the effect of heat transfer during the melting process, and speed up the phase change process of the composite materials. The solidification temperature of $LiNO_3$–NaCl binary mixed molten salt is 222.4 ℃. It only decreases 1.2 ℃ compared to its melting point, which demonstrates that $LiNO_3$–NaCl has very small supercooling degree. The solidification temperatures of LNE samples are all below their melting temperatures and are obviously lower than that of $LiNO_3$–NaCl binary mixed molten salt. For LNE, the supercooling degrees are between 7 and 11.9 ℃, which are higher than that of $LiNO_3$–NaCl binary mixed molten salt. The possible reason is that the pressure in the holes decreases during the solidification process of composite molten salt. Then the solidification temperature of the composites decreases.

By calculating the area of the endothermic peak and the exothermic peak of the sample DSC curve, the enthalpy of melting and solidification of the composite PCM can be obtained. Table 2 shows the solidification enthalpy is about 96 % of the melting enthalpy. The possible reason may be that the supercooling phenomenon causes the decrease of the enthalpy.

The phase change enthalpy comes from binary mixed molten salt $LiNO_3$–NaCl, EG does not absorb or release heat during the phase change process. Figure 3 shows the

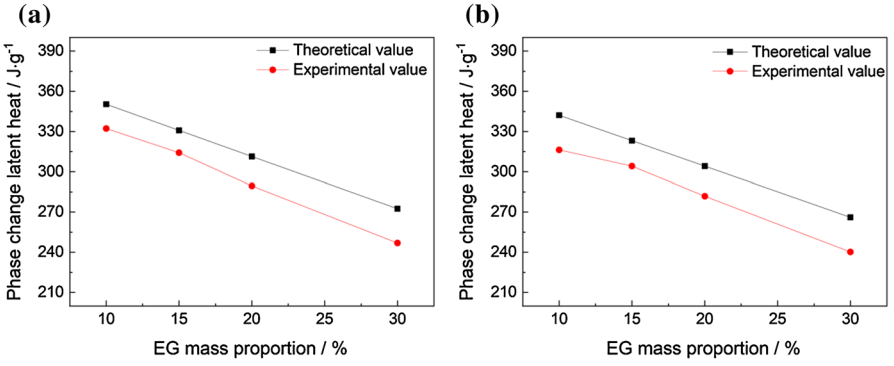

Fig. 3 Comparison of the theoretical and experimental phase change enthalpy for LNE (a) melting process (b) solidification process

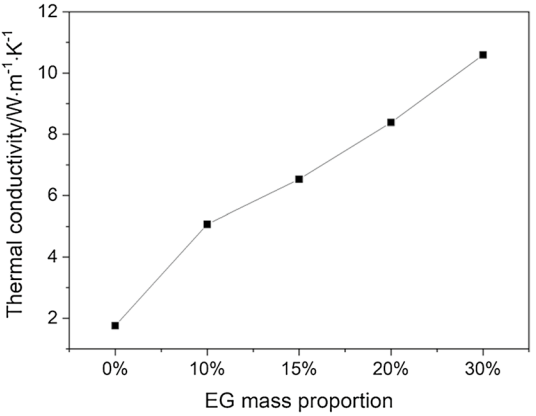

Fig. 4 The thermal conductivities of composites with different EG mass proportions

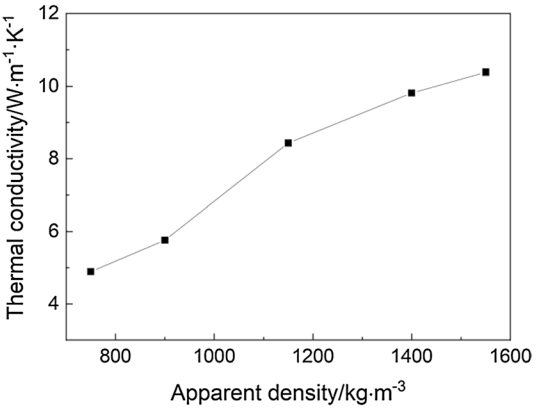

Fig. 5 Thermal conductivity of the PCM with 15 wt% EG at different apparent density

comparison between experimental measured phase change enthalpy and theoretical calculation value. The theoretical calculation value is equal to the latent heat of the heat storage material multiplied by the mass ratio of the heat storage material to the composite heat storage material. We can see that the experimental melting enthalpy and solidification enthalpy are both lower than theoretical values. The difference will expand with the increase of EG mass proportion. The first possible reason is that some PCM adheres to the container during the preparation process, and the effect becomes bigger with the decrease of PCM mass proportion. The second possible reason is that the uncontrolled error can be caused by the deliquescence of the mixed molten salt. According to test results, the adsorption ratio of the mixed salt exceeds 90 % to 95 %. EG is a good carrier for the preparation of composite PCMs.

3.3 Thermal Conductivity of Composite PCM

The thermal conductivities of composite PCMs are shown in Figs. 4 and 5. The apparent density is 1000 kg·m^{-3} for all the samples in Fig. 4. The thermal

conductivity increases rapidly with the increase of EG mass proportion. The average thermal conductivity of $LiNO_3$–NaCl is only 1.754 $W{\cdot}m^{-1}{\cdot}K^{-1}$. The thermal conductivities of the composites with 10 %, 15 %, 20 %, 30 % EG are 5.066 $W{\cdot}m^{-1}{\cdot}K^{-1}$, 6.532 $W{\cdot}m^{-1}{\cdot}K^{-1}$, 8.386 $W{\cdot}m^{-1}{\cdot}K^{-1}$, 10.593 $W{\cdot}m^{-1}{\cdot}K^{-1}$, about 2.89–6.04 times that of $LiNO_3$–NaCl binary mixed molten salt. Besides adsorbing PCM, EG can also improve the thermal conductivity of the mixed molten salt and heat storage efficiency significantly.

The relationship between apparent density and thermal conductivity is shown in Fig. 5 for the sample with 15 wt% EG mass proportion. The thermal conductivity is closely related to the apparent density. The thermal conductivity increases from 4.891 to 10.387 $W{\cdot}m^{-1}{\cdot}K^{-1}$ when the apparent density increases from 750 to 1550 $kg{\cdot}m^{-3}$. The results of this study are consistent with those of literature [23]. EG is a porous structural material with great compressibility. When the apparent density increases, the porosity decreases. As the contact area of composite particles increases, more effective heat conduction paths are formed within the composites.

3.4 Thermal Stability Test Results

The composite PCM of 85 wt% $LiNO_3$-NaCl/15 wt% EG is selected for the cyclic thermal stability test. 10 consecutive DSC tests were performed on the same sample under the same test conditions. The DSC curve of cyclic thermal stability is shown in Fig. 6. The related thermal physical property test data of the composite PCM during the heating and cooling process are shown in Table 3. It shows that the peak shape and peak position of the endothermic melting peak and exothermic solidification peak of the composite PCM change little during the 10 cycles. The phase change temperature of the composite PCM is about 221 ℃, and the latent heat of fusion Hm and the latent heat of solidification Hs are about 316 $J{\cdot}g^{-1}$ and 307 $J{\cdot}g^{-1}$, respectively. It shows that the composite PCM has stable performance during the 10 cycles of the experiment.

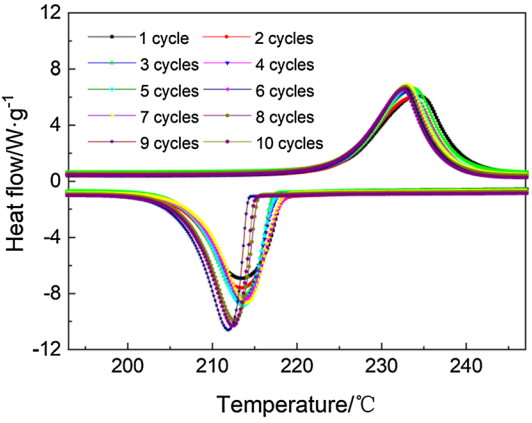

Fig. 6 Thermal cycle DSC curve of composite phase change material

Table 3 Cyclic thermal stability test results of composite phase change materials

Number of thermal cycles	The melting process			The solidification process		
	T_m (℃)	$T_{peak\text{-}m}$ (℃)	H_m (J·g^{-1})	T_s (℃)	$T_{peak\text{-}s}$ (℃)	H_s (J·g^{-1})
1 cycle	221.1	228.6	314.1	214.9	211.6	311.6
2 cycles	220.6	228.0	315.9	214.8	211.7	309.9
3 cycles	221.4	227.9	320.2	213.6	211.6	312.4
4 cycles	220.7	227.5	317.9	214.0	212.0	311.8
5 cycles	221.3	227.6	321.7	213.8	212.1	310.9
6 cycles	220.8	227.2	319.6	214.8	212.1	310.4
7 cycles	221.5	227.3	314.1	214.5	212.4	309.9
8 cycles	221.0	227.2	317.1	212.1	211.3	311.3
9 cycles	221.2	227.2	311.0	211.0	210.6	301.4
10 cycles	220.8	226.9	312.7	211.8	211.2	302.2

4 Conclusions

LNE were prepared using static melt adsorption method. The thermal physical properties were tested and analyzed by XRD, DSC and Hot Disk thermal constant analyzer. The main conclusions are as follows:

1. EG with high thermal conductivity keeps good thermal chemical stability under LNE preparation process. It has good chemical compatibility with $LiNO_3$–NaCl mixed molten salt. The composite PCM has stable performance.
2. EG has the effect of heterogeneous nucleation, it increases the number of nucleation points in the composites and reduces the mixed molten salt grain size. The melting temperature of the composite PCM drops by 0.6–3.5 ℃. The solidification temperature of the composites reduces more, their supercooling degree is between 7 and 11.9 ℃. The possible reason is that the pressure in EG hole decreases during the solidification process of molten salt, leading to the decrease of solidification temperature.
3. The phase change enthalpy of composite PCMs reduces with the increase of EG mass proportion. The melting latent heats are between 246.9 and 332.2 J·g^{-1} and the solidification latent heats are between 240.2 and 316.3 J·g^{-1}. It demonstrates that the composite materials have good heat storage performance. The adsorption ratio of PCM exceeds 90 % to 95 % for all the samples. EG is a good carrier for the preparation of composite PCMs.
4. The thermal conductivity of composite PCMs significantly increases with the increase of EG mass proportion. The thermal conductivities of the composites with 10 wt%, 15 wt%, 20 wt%, 30 wt% EG are 5.066 m^{-1}·K^{-1}, 6.532 W·m^{-1}·K^{-1}, 8.386 W·m^{-1}·K^{-1}, 10.593 W·m^{-1}·K^{-1}, about 2.89 to 6.04 times that of $LiNO_3$–NaCl binary mixed molten salt. The thermal conductivity increases with the increase of the apparent density.

5. Considering the heat storage capacity, thermal conductivity, and adsorption ratio, 85 wt% $LiNO_3$–NaCl/15 wt% EG composite PCM has relatively good overall performance.

Acknowledgments This research is supported by the Science and Technology Commission of Shanghai Municipality under the Contract No. 20dz1205208, which is gratefully acknowledged by the authors.

References

1. L. Miró, J. Gasia, L.F. Cabeza, Appl. Energy. **179**, 284 (2016)
2. Z. Yang, S.V. Garimella, Sol Energy. **84**, 974 (2010)
3. S. Guillot, A. Faik, A. Rakhmatullin, J. Lambert, E. Veron, P. Echegut, C. Bessada, N. Calvet, X. Py, Appl. Energy. **94**, 174 (2012)
4. W. Han, C. Ge, R. Zhang, Z. Ma, L. Wang, X. Zhang, Appl. Energy. **238**, 942 (2019)
5. Z. Qian, H. Shen, X. Fang, L. Fan, N. Zhao, J. Xu, Energy Build. **158**, 1184 (2018)
6. M.E. Navarro, A. Palacios, T. Hughes, C. Connolly, H. Uppal, L. Cong, X.Z. Lei, G. Qiao, G.H. Leng, Y.L. Ding, Energy Storage Sci. Technol. **6**, 688 (2017)
7. N. Putra, S. Rawi, M. Amin, E. Kusrini, E.A. Kosasih, T.M. Indra Mahlia, J Energy Storage. **21**, 32 (2019)
8. X. Huang, G. Alva, Y. Jia, G. Fang, Renew Sustain Energy Rev. **72**, 128 (2017)
9. Y. Li, G. Yue, Y.M. Yu, Q.Z. Zhu, Energy **196**, 117067 (2020)
10. J.W. Liu, Q.H. Wang, Z.Y. Ling, X.M. Fang, Z.G. Zhang, Sol. Energy Mater Sol. Cells. **169**, 280 (2017)
11. D. Feng, Y. Feng, L. Qiu, P. Li, Y. Zang, H. Zou, Z. Yu, X. Zhang, Renew. Sust. Energy Rev. **109**, 578 (2019)
12. Q. Zhang, H. Wang, Z. Ling, X. Fang, Z. Zhang, Sol. Energy Mater Sol. Cells. **140**, 158 (2015)
13. S. Wang, P. Qin, X. Fang, Z. Zhang, S. Wang, X. Liu, Sol Energy. **99**, 283 (2014)
14. Y. Zhao, R. Wang, L. Wang, N. Yu, Energy **70**, 272 (2014)
15. X. Xiao, P. Zhang, M. Li, Energy Convers Manag. **105**, 272 (2015)
16. Y.F. Li, D. Zhang, J. Funct. Mater. **10**, 1451 (2013). [**in Chinese**]
17. Y.Q. Zhao, L. Jin, B.Y. Zou, G. Qiao, T.T. Zhang, L. Cong, F. Jiang, C. Li, Y. Huang, Appl. Therm. Eng. **171**, 115015 (2020)
18. D.G. Atinafu, Y.S. Ok, H.W. Kua, S. Kim, Appl. Therm. Eng. **181**, 115960 (2020)
19. D.L. Feng, Y.Y. Zang, P. Li, Y.H. Feng, Y.Y. Yan, X.X. Zhang, Compos. Sci. Technol. **210**, 108832 (2021)
20. Y. Li, P. Li, Q.Z. Zhu, Q.F. Li, Int. J. Thermophys. **37**, 104 (2016)
21. Y. Li, P. Li, Q.Z. Zhu, Y.M. Yu, J. Chin. Ceramic Soc. **46**, 624 (2018). [**in Chinese**]
22. Y. Li, C.G. Wang, G.Y. Liu, Q.Z. Zhu, Z.Z. Qiu, Int. J. Thermophys. **40**, 41 (2019)
23. Z.W. Huang, D.H. Zhai, X.N. Gao, Appl. Therm. Eng. **86**, 309 (2015)